

Signatures of Dynes superconductivity in the THz response of ALD-grown NbN thin films

Frederik Bolle¹, Yayi Lin¹, Ozan Saritas¹, Martin Dressel^{1,2}, Ciprian Padurariu³, Sahitya Varma Vegesna^{4,5}, Nitesh Yerra⁴, Heidemarie Krüger^{4,5}, and Marc Scheffler^{1,2}

^{1,1} *Physikalisches Institut, Universität Stuttgart, 70569 Stuttgart, Germany*

² *Center for Integrated Quantum Science and Technology (IQST), Universität Stuttgart, 70569 Stuttgart, Germany*

³ *Institute for Complex Quantum Systems and IQST, Universität Ulm, 86069 Ulm, Germany*

⁴ *Leibniz Institute of Photonic Technology, 07745 Jena, Germany*

⁵ *Institute for Solid State Physics, Friedrich-Schiller Universität Jena, 07743 Jena, Germany*

(Dated: February 17, 2026)

The frequency-dependent complex optical conductivity $\hat{\sigma}(f)$ reflects key properties of superconductors, such as the energy gap 2Δ in the density of states (DOS) and the superfluid density n_s . For disordered superconductors, $\hat{\sigma}(f)$ often can be described within Bardeen-Cooper-Schrieffer (BCS) theory, while in corresponding tunneling experiments, deviations in the observed DOS typically require modelling by the phenomenological Dynes formula. The implications of such Dynes DOS for optics were rarely discussed so far. Here we probe the terahertz $\hat{\sigma}(f)$ of superconducting NbN thin films with thicknesses ranging from 4.5 to 20 nm, which were grown by atomic layer deposition (ALD). Our frequency range from 0.3 to 2.1 THz covers energies below and above 2Δ . For 20 nm thick NbN, we find in $\hat{\sigma}(f)$ distinct deviations from the BCS model, including a step-like characteristic in the absorption at Δ_0 , i.e. half the zero-temperature spectral gap. These observations can be fully captured by Dynes electrodynamics with a small and temperature-independent pair-breaking rate $\Gamma \sim 0.036\Delta_0$. For the other films, we also observe signs of Dynes electrodynamics, and we discuss the evolution of $2\Delta_0$, $n_{s,0}$, and Γ as function of film thickness.

I. INTRODUCTION

When a conventional s-wave superconductor is cooled below its critical temperature T_c , a gap of size 2Δ opens up in the density of states (DOS) due to the formation of Cooper pairs. According to the Bardeen-Cooper-Schrieffer (BCS) theory, Cooper pairs can be broken by thermal excitation or radiation with sufficient energy $E > 2\Delta$. Therefore, at very low temperatures $T \ll T_c$, no absorption channels exist within the superconducting gap $2\Delta_0 = 2\Delta(T = 0)$, since the DOS is exactly zero.

Experimentally, the energy-dependent density of states $N(E)$ of a superconductor can be probed by means of tunneling spectroscopy, either using scanning tunneling microscopy in spectroscopy mode or using junctions with thin dielectric films as tunneling barriers. In the framework of disordered and ultra-thin superconductors, such measurements typically reveal a non-zero DOS at zero bias even at temperatures far below the critical temperature [1–3] and in zero magnetic field, which is not accounted for within the BCS model. To quantitatively describe the emergence of these in-gap states, one can employ the Dynes model [4], which introduces a phenomenological scattering rate Γ that quantifies additional pair-breaking mechanisms in superconductors

$$N(E) = N_0 \operatorname{Re} \left(\frac{E + i\Gamma}{\sqrt{(E + i\Gamma)^2 - \Delta^2}} \right). \quad (1)$$

Here N_0 is the normal-state DOS at the Fermi level, and Δ is the ideal superconducting gap within the BCS model. These modifications to the single-particle DOS have direct consequences for the dynamical conductivity

[5], including a characteristic step-like absorption feature at half of the spectral gap Δ . Despite the wide use of the Dynes model in describing tunneling data [1, 2, 6, 7], a direct observation of this postulated absorption step by optical means has not been reported yet.

The superconducting electrodynamics of sputtered or pulsed laser deposited NbN thin films have widely been investigated [8–17]. In this work, we study a series of atomic layer deposited NbN thin films [18, 19] using terahertz (THz) spectroscopy to directly probe the complex conductivity $\hat{\sigma}(f)$ over a broad range of frequencies f and temperatures T .

II. EXPERIMENT

NbN films of thicknesses d ranging from 4.5 to 20 nm were deposited on 530 μm thick $10 \times 10 \text{ mm}^2$ R-plane sapphire (Al_2O_3) using atomic layer deposition (ALD). For more details regarding the precise deposition parameters and used precursors, consider the report by Linzen *et al.* [18]. Various sample properties are listed in Table I. As a first characterization of the thin films, transport measurements were conducted in van der Pauw geometry to obtain the transition temperature T_c and normal-state resistivity ρ_0 . To study the optical response in the THz regime [14], a commercial THz time-domain spectrometer (TeraPulse 4000) as well as a frequency-domain spectrometer were used in transmission geometry. In the latter, frequency-tunable backward wave oscillators (BWO) generate monochromatic, coherent light in the THz regime, which is transmitted through the sample and detected using a Golay cell or a ^4He cooled bolometer

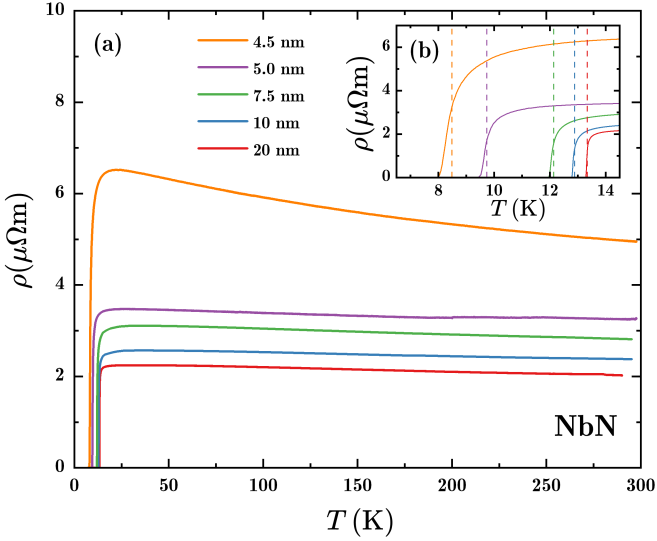


FIG. 1. The main panel (a) shows the temperature-dependent resistivity $\rho(T)$ for all studied films, while the inset (b) displays a magnified view of the behavior near the superconducting transition temperature T_c , where T_c is defined via the 50% criterion with respect to the maximum of the normal-state resistivity, as indicated by dashed lines.

[14]. This approach has been used extensively to study the low-energy optical conductivity of superconductors [20–22]. The photon energy $E = hf$, with Planck’s constant h , is the relevant energy scale of the optical experiments below. For convenience and closer connection to the THz experiments with f as common tuning parameter, we will relate energy scales such as Δ to either E or f , depending on the context.

III. RESULTS

A. Transport properties and optical conductivity

Results of transport measurements, displayed in Figure 1, show that all five films become superconducting with critical temperatures ranging from 8.5 to 13.3 K. With decreasing film thickness, the normal-state resistivity increases, and the critical temperature is suppressed significantly [23–26]. Additionally the width of the transition increases as the film dimensions become increasingly two-dimensional.

The complex optical conductivity of the 20 nm NbN film obtained using THz time-domain spectroscopy (TDS) is shown in Figure 2. Above the critical temperature of around 13.3 K, the film shows a frequency-independent real part σ_1 of the complex optical conductivity $\hat{\sigma} = \sigma_1 + i\sigma_2$, indicating a normal-state Drude-type scattering rate Γ_n far outside our accessible spectral range, as expected for a dirty superconductor above T_c . Below the critical temperature, the low-frequency σ_1 is significantly suppressed due to the pairing of elec-

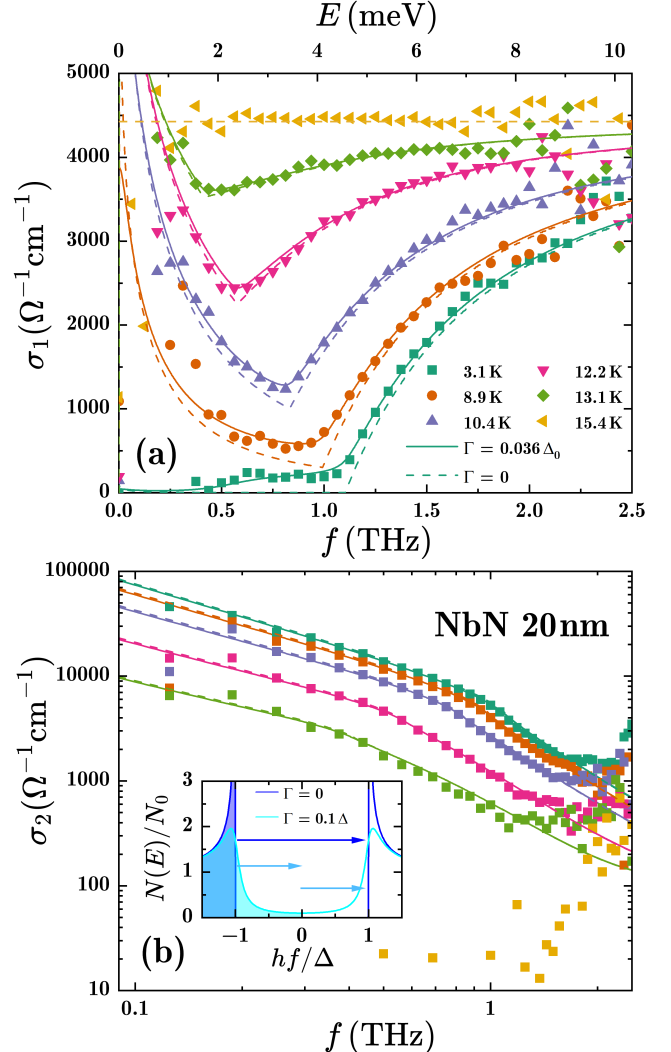


FIG. 2. Complex optical conductivity $\hat{\sigma} = \sigma_1 + i\sigma_2$ of a 20 nm NbN thin film with $T_c \approx 13.3$ K, obtained with THz time-domain spectroscopy (TDS), where panel (a) shows the real part σ_1 on linear scales and (b) the imaginary part σ_2 on logarithmic scales. Solid lines represent fits according to the Dynes model [5] with a finite and constant pair-breaking rate of $\Gamma = 0.036 \Delta_0$, while dashed lines are calculated according to the Mattis-Bardeen model [27], corresponding to $\Gamma = 0$. The strongest deviations between the Dynes and Mattis-Bardeen models occur near the temperature-dependent minimum of $\sigma_1(f)$. The normal-state conductivity at 15.4 K is sketched as a dashed, horizontal line in (a) and corresponds to the value $\sigma_{dc} = 4460 \Omega^{-1} \text{cm}^{-1}$ obtained from transport measurements. The inset in (b) shows the superconducting density of states near the Fermi energy in the limit $T = 0$. In the BCS case ($\Gamma = 0$), only excitations with $hf > 2\Delta$ are allowed (dark blue arrow). In the Dynes case (here: $\Gamma = 0.1\Delta$), also excitations at lower energies are possible, and the transitions indicated by light blue arrows, with $hf = \Delta$, lead to the step near Δ in $\sigma_1(f)$.

TABLE I. Summary of characteristic material properties of superconducting NbN samples such as the thickness d , the sheet resistance $R_{s,DC}$, the critical temperatures obtained from DC $T_{c,DC}$ and THz measurements $T_{c,THz}$, the spectral gap $2\Delta_0$, the coupling ratio $2\Delta_0/(k_B T_{c,DC})$, the superfluid density $n_{s,0}$, the London penetration depth $\lambda_{L,0}$, the sheet kinetic inductance $L_{kin,0}^{\square}$, and the pair-breaking rate Γ/Δ_0 . $T_{c,DC}$ and $R_{s,DC}$ have been obtained through DC transport measurements. For samples with $d < 7.5$ nm, Δ_0 has been solely determined from frequency-domain measurements.

| d [nm] | $R_{s,DC}$ [Ω/sq] | ρ_{dc} [$\mu\Omega\text{m}$] | $T_{c,DC}$ [K] | $T_{c,THz}$ [K] | $2\Delta_0$ [meV] | $2\Delta_0$ [THz] | $2\Delta_0/(k_B T_{c,DC})$ | $n_{s,0} \cdot 10^{25}$ [m^{-3}] | $\lambda_{L,0}$ [nm] | $L_{kin,0}^{\square}$ [pH/sq] | Γ/Δ_0 |
|-------------|--------------------------------------|--|-------------------|--------------------|----------------------|----------------------|----------------------------|--|-------------------------|--|-------------------|
| 4.5 | 1445 | 6.50 | 8.49 | 8.63 | 0.605 | 2.50 | 3.42 | 3.04 | 848 | 259 | 0.028 |
| 5 | 695 | 5.55 | 9.74 | 9.74 | 0.707 | 2.92 | 3.49 | 5.08 | 740 | 139 | 0.019 |
| 7.5 | 413 | 3.10 | 12.14 | 11.63 | 0.971 | 4.02 | 3.84 | 10.85 | 532 | 43.6 | 0.017 |
| 10 | 256 | 2.55 | 12.89 | 12.72 | 1.073 | 4.44 | 4.00 | 14.55 | 493 | 24.4 | 0.010 |
| 20 | 112 | 2.23 | 13.34 | 13.60 | 1.124 | 4.65 | 4.05 | 16.87 | 443 | 10.5 | 0.036 |

trons into Cooper pairs. The corresponding minimum in σ_1 is readily identified as the spectral gap 2Δ above which Cooper pairs are broken up by incoming THz photons into individual quasiparticles. Simultaneously, a clear $1/f$ dependence develops in the imaginary part σ_2 for frequencies below the spectral gap, which increases in magnitude for lower temperatures [28]. To describe the dynamical conductivity, we first use the model by Zimmermann *et al.* [27], which is a description of the Mattis-Bardeen equations generalized for samples of arbitrary purity. Motivated by the frequency-independent normal-state conductivity, we set the impurity parameter $y = \hbar\Gamma_n/(2\Delta) = 500$ (impure limit) [27], with reduced Planck's constant \hbar . The model fits our data reasonably well and allows us to extract superconducting properties, such as the temperature-dependent spectral gap $2\Delta(T)$ and the superfluid density $n_s(T)$, which will be discussed below. All obtained parameters from transport and optical measurements are summarized in Table I.

B. Signatures of Dynes superconductivity

Considering the σ_1 spectrum at lowest temperature $T = 3.1$ K in Figure 2, we find that the Zimmermann fit does not fully describe the data. We observe an onset of absorption starting at half the spectral gap 2Δ , which is not captured by the standard BCS model for the dynamical conductivity. To describe the additional losses seen in the experiment, we use the model for the optical conductivity of superconductors with pair-breaking processes as described by Herman and Hlubina [5] and based on the Dynes DOS, Equation 1, as illustrated in the inset of Figure 2(b). This modification leads to a smearing of the energy gap together with the emergence of a distinct absorption step at Δ , which can be understood when considering the modified DOS. Due to the gapless nature of Dynes superconductors, absorption is possible at arbitrarily low frequencies similar to a normal metal. The joint density of states and correspondingly $\sigma_1(f)$ increase at both steps: one at Δ (corresponding to excitations from the DOS maximum around $-\Delta$ to the Fermi energy E_F at $E_F = 0$ or from E_F to the DOS maximum around $+\Delta$) and the other at 2Δ (cor-

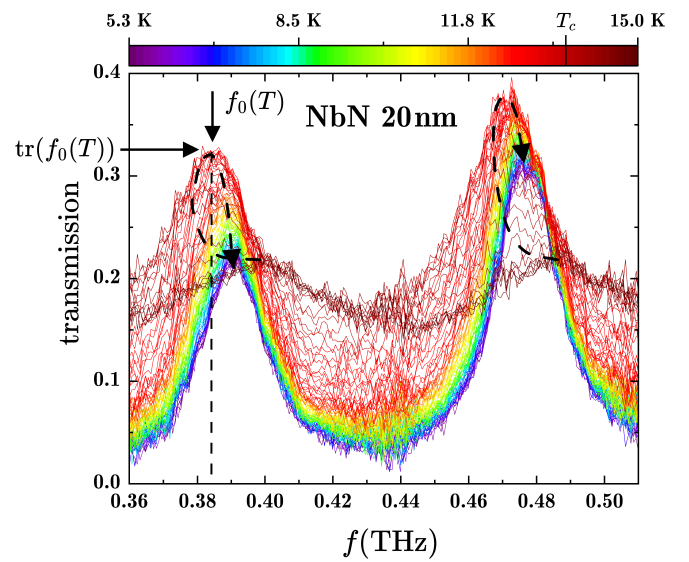


FIG. 3. Fabry-Pérot (FP) resonances, observed for numerous temperatures in THz frequency-domain spectroscopy (FDS) on 20 nm NbN for two modes, with FP frequencies $f_{0,n} = 0.4$ and 0.49 THz in the metallic state at $T = 15$ K. Arrows indicate the positions of the temperature-dependent resonance frequency and its corresponding transmission value. Additionally, dashed arrows are guides to the eye to indicate the shift of the modes as the temperature is lowered.

responding to excitations between the two DOS maxima at $-\Delta$ and $+\Delta$). We model our conductivity spectra with a two-parametric fit for all temperatures to obtain the temperature-dependent energy gap $\Delta(T)$ and the pair-breaking rate $\Gamma(T)$, which is basically constant $\Gamma = 0.036 \Delta_0$, as shown in Figure 5. By using the Dynes model we can achieve a near-perfect description of the dynamical conductivity in Figure 2, capturing the step-like feature observed at 3.1 K, as well as the systematic deviation at higher temperatures.

To further support this observation of Dynes superconducting THz electrodynamics of our films, we turn to frequency-domain spectroscopy (FDS). As an example the raw transmission spectrum of the 20 nm NbN film for numerous temperatures is shown in Figure 3.

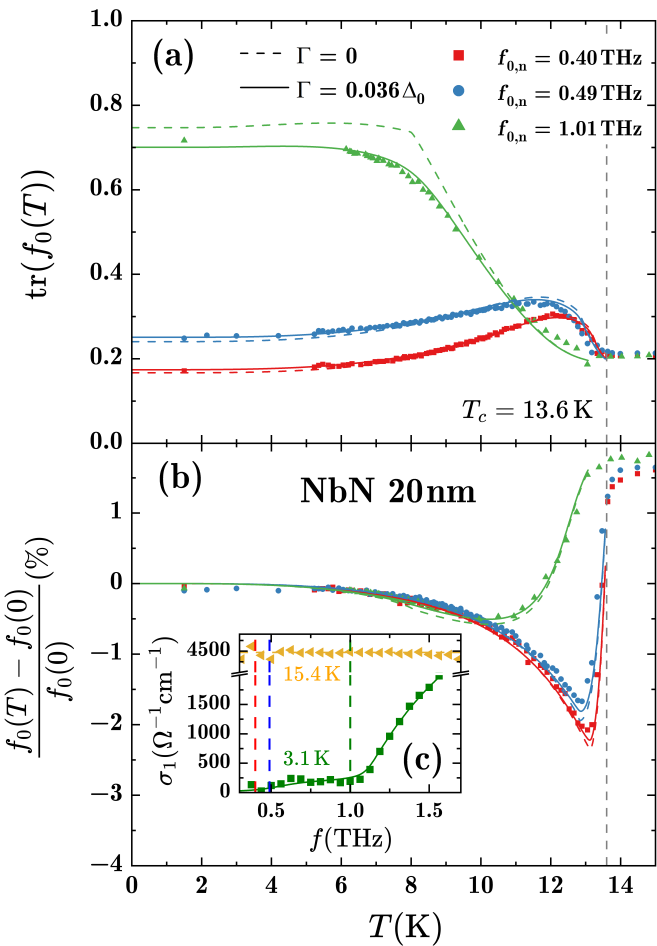


FIG. 4. Frequency-domain spectroscopy (FDS) studies of the temperature-dependent transmission $\text{tr}(f_0(T))$ at temperature-dependent resonance frequency $f_0(T)$ and fractional resonance frequency shift $\frac{f_0(T) - f_0(0)}{f_0(0)}$ displayed in panel (a) and (b) respectively. Solid lines represent fits according to the Dynes model [5] with a finite pair-breaking rate of $\Gamma = 0.036 \Delta_0$, while dashed lines are modeled according to the Mattis-Bardeen model [27], corresponding to $\Gamma = 0$. The vertical line at $T = 13.6 \text{ K}$ indicates T_c obtained from the THz measurements. The inset (c) shows the real part of the optical conductivity σ_1 , obtained from TDS, at 3.1 K and in its normal state at 15.4 K , with dashed vertical lines indicating the frequency positions of the Fabry-Pérot modes studied by FDS.

We observe the periodic Fabry-Pérot (FP) transmission pattern, caused by constructive and destructive interference in the dielectric substrate and modified by the temperature-dependent superconducting properties of the thin film. As the film is cooled below T_c , strong changes can be observed in absolute transmission and in resonance frequency. We treat each FP mode as a resonating mode, with a characteristic resonance frequency f_0 and an absolute transmission at the maximum $\text{tr}(f_0)$. Here the THz photon energy is comparable to Δ_0 , and

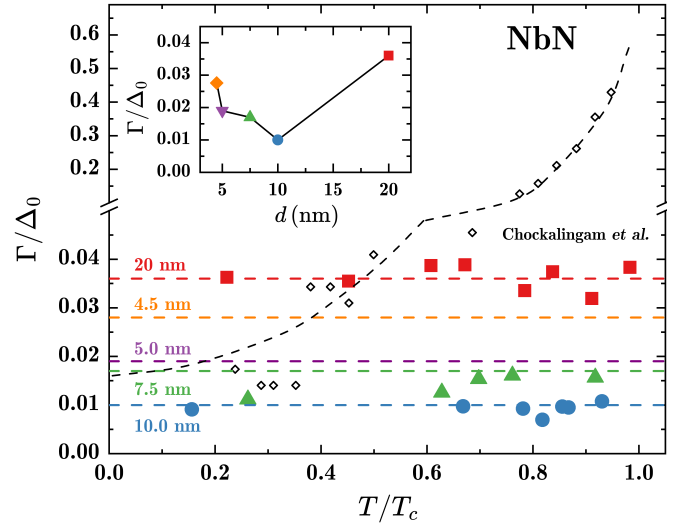


FIG. 5. Pair-breaking rates Γ for five NbN samples normalized to their zero-temperature energy gap Δ_0 , from both TDS (discrete temperature points) and FDS (dashed lines) studies. For comparison, pair-breaking rates obtained by Chockalingam *et al.* [1] from tunneling spectroscopy measurements on NbN are shown as open diamonds with a dashed line as a guide to the eye. The inset displays Γ/Δ_0 , as determined from FDS, for the different film thicknesses.

the in-gap absorption seen previously in TDS should also appear in this FDS experiment. The result of this investigation for three FP modes is shown in Figure 4, with the absolute transmission in panel (a) and the normalized change in resonance frequency in panel (b). We model the FP transmission pattern using an analytic expression for the transmission coefficient [28] combined with the Dynes model for optical conductivity. Motivated by the temperature-independent pair-breaking rate seen by TDS, we assume a constant $\Gamma(T) = \Gamma$. Other characteristic parameters, such as the spectral gap and normal-state conductivity correspond to the ones obtained from TDS. As evident from Figure 4, we observe a very convincing match between theory and experiment, fully reproducing the temperature and frequency dependence of the modes. As the film is cooled below T_c , a gap opens up leading to a suppression of $\sigma_1(f)$. As a consequence, for modes close to the spectral gap $2\Delta_0$, in our case for $f = 1 \text{ THz}$, where the transmission is dominated by changes in σ_1 , the transmission strongly increases upon cooling. For lower frequency modes, an interplay between σ_1 and σ_2 leads to the emergence of a distinct maximum of the transmission just below the critical temperature (not to be confused with the coherence peak in $\sigma_1(T)$ at low frequencies [29]). This maximum is at much lower temperatures and much weaker for the mode at 1 THz , where additionally a clear change of slope in the absolute transmission (best seen in the Mattis-Bardeen prediction at around $T = 8 \text{ K}$) indicates the crossing of the FP mode with the kink in $\sigma_1(f)$ at the spectral gap $2\Delta(T)$. For the highest frequency mode at around 1 THz ($E \approx 1.8\Delta_0$), the

absolute transmission of the mode clearly shows strong deviations from the BCS prediction, indicating the existence of an additional pair-breaking mechanism, which leads to the excess sub-gap conductivity. The magnitude of the pair-breaking rate determined from this FP investigation in FDS, $\Gamma = 0.036 \Delta_0$, matches TDS on the same film and confirms the temperature-independence of the pair-breaking rate. Combining both TDS and FDS studies, we plot in Figure 5 the obtained pair-breaking rates Γ for the five NbN samples, normalized to Δ_0 . For all of them we find temperature-independent Γ . This is in contrast to tunneling spectroscopy results on a NbN film with comparable level of disorder previously reported by Chockalingam *et al.* [1], which we have included in Figure 5 as comparison. For low temperatures the magnitude of the pair-breaking rate from THz and tunneling measurements are similar, but strong deviations emerge for higher temperatures, where tunneling measures values of the pair-breaking rate of up to 50% of Δ_0 , while the values from our optical measurements remain small and temperature-independent. One relevant parameter here is the size of the volume that is probed, as local changes in resistivity can lead to an inhomogeneous energy landscape of the superconductor [30]. In contrast to scanning tunneling spectroscopy with sub-nm spatial resolution, both our THz study and the tunneling experiment in [1] average over comparable lateral dimensions defined by the THz spot size (comparable to wavelength) and the junction area, respectively. One difference, though, is the spectroscopy probing depth: while THz transmission probes the complete film thickness and thus is mostly sensitive to the bulk of the NbN thin film, tunneling is inherently surface sensitive and in the case of thin-film junctions might also be affected by details of the barrier. Another, generally relevant possible cause for observed differences in the Dynes scattering parameter are differences in thin-film growth, which affect the microscopic film structure.

C. Superconducting properties

Lastly we discuss the superconducting properties, in particular the energy gap and superfluid density shown in Figure 6(a) and (c), respectively, for the five NbN samples. To determine the density of superconducting charge carriers, we utilize that the optical conductivity $\hat{\sigma}(f)$ obeys Kramers-Kronig relations, therefore we can relate the magnitude of the δ -distribution in $\sigma_1(f = 0)$ to the imaginary part $\sigma_2(f)$

$$n_s = \frac{2\pi m^*}{e^2} \lim_{f \rightarrow 0} f \sigma_2(f), \quad (2)$$

where $m^* = m_e$ is the effective mass of quasiparticles in NbN. The temperature dependence of the energy gap is well described within the BCS model. For thicker films, the gap ratio $2\Delta_0/(k_B T_c)$ of our NbN films is significantly

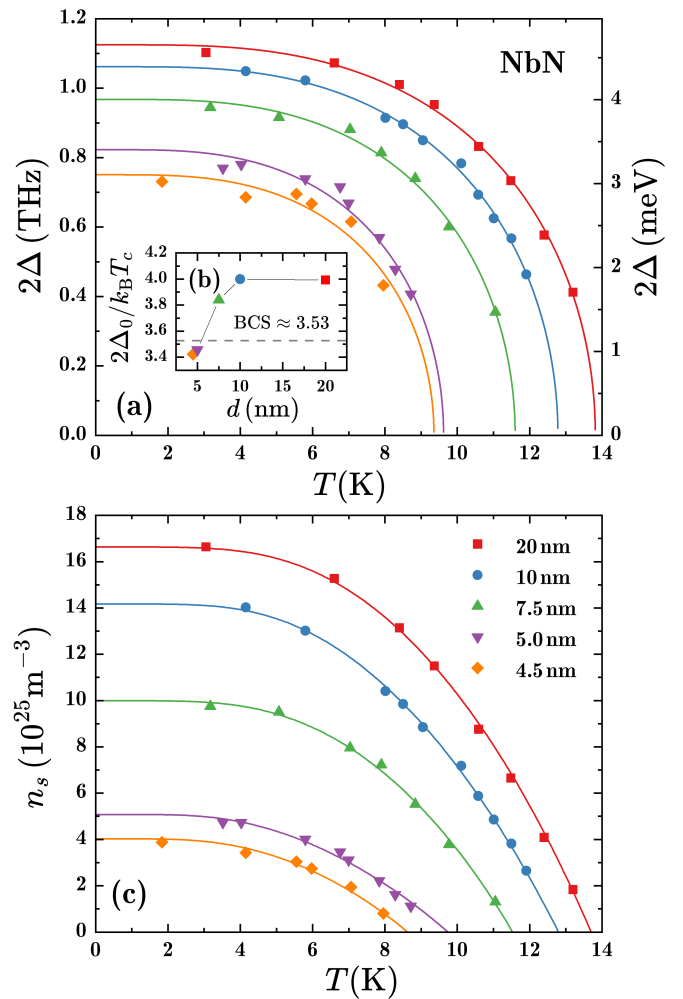


FIG. 6. (a) Temperature-dependent superconducting energy gap $2\Delta(T)$ and (c) superfluid density $n_s(T)$ obtained from using the Dynes model. The temperature dependence of the energy gap is modeled using a BCS approximation $\Delta(T) = \Delta(0) \tanh(1.74\sqrt{T_c/T} - 1)$ while the superfluid density is modeled using the procedure described in [31]. The inset in (b) depicts the gap ratio $\frac{2\Delta_0}{k_B T_c}$ with the dotted line representing the weak coupling BCS limit.

higher (≈ 4.0) than the weak coupling limit of 3.528, indicating strong electron-phonon coupling [9]. Reducing the film thickness suppresses its superconducting properties due to increased electron-electron repulsion which suppresses the phonon-mediated attractive pairing. To classify our results for the coupling ratio, we consider the abundant literature on NbN, with works reporting conflicting behaviors as T_c is suppressed with increasing disorder, typically in conjunction with reduced film thickness [1, 16, 22, 32]. In particular the coupling ratio, which is directly related to the magnitude of the energy gap and its critical temperature, can show varying behaviors as disorder is increased. A report by Chand *et al.* reveals the complex nature of the phase diagram of strongly disordered NbN thin films [33]. As one in-

creases the disorder of the system, first superconductivity is suppressed due to gradual reduction of pairing interactions after which an intermediate disorder regime follows, which is governed by the suppression of the superfluid stiffness J . This intermediate regime is concomitant with the emergence of a pseudo-gap state surviving even above the critical temperature, which persists until (maybe even beyond) the destruction of superconductivity at $k_f l \approx 1$, with Fermi wavevector k_f and mean free path l . Beyond critical levels of disorder, the insulating regime of NbN is characterized by incoherent superconducting islands, reminiscent of the situation in other disordered superconductors such as TiN [34], InO_x [35] and granular aluminum [20]. The rich phase diagram of NbN indicates that multiple processes of both fermionic (electronic interactions) and bosonic nature (phase coherence between Cooper pairs) play a role when approaching the transition to its disorder-induced insulating state. From the continuous reduction of the coupling ratio and the absence of phenomena indicating a pseudo-gap, we conclude that the suppression of superconductivity within the disorder regime of the films studied in this work is mainly governed by electronic interactions, e.g. they lie in the fermionic regime of the superconductor-insulator transition of NbN.

IV. DISCUSSION

We find that for the NbN films under study, conventional BCS electrodynamics cannot describe the THz data whereas inclusion of a finite Dynes pair-breaking parameter Γ leads to excellent agreement. While the Dynes formula has been useful as a phenomenological model that yields an in-gap density of states, the microscopic origin of the Dynes parameter remains unclear. A number of competing phenomena have been proposed to contribute to the Dynes parameter. Two main mechanisms are valid in most conventional superconducting materials: (i) inelastic electron scattering that leads to Cooper-pair breaking [36, 37] and (ii) magnetic scattering [5, 38, 39] that lowers the local single-particle excitation energy. Other mechanisms have also been identified in materials with spatially inhomogeneous or exotic order parameters, or in materials with different superconducting order parameters in different bands [6]. Inelastic electron scattering can occur either due to electron-phonon scattering, or due to electron-electron scattering. Since inelastic electron scattering is also responsible for the normal-state conductance of a metal, the resulting contribution to the Dynes parameter is expected to have a similar magnitude and temperature dependence when extrapolated above the critical temperature. From the temperature-independence of the pair-breaking rate seen by our two independent THz measurement procedures, we infer that inelastic electron scattering processes are not the prevailing explanation for the emergence of in-gap states in NbN. Magnetic scattering at a localized

impurity induces a single, discrete, and well-localized Yu-Shiba-Rusinov state inside the superconducting gap, and not a continuum of in-gap states. However, it has been shown that hybridization of such states due to a random density of magnetic scattering centers can lead to an in-gap density of states consistent with the Dynes formula [5, 38, 39]. Additionally, a recent theoretical work by Yang and Wu [40] predicts an interband transition between Shiba impurity bands across the energy gap, which leads to an optical absorption feature close to Δ . In tunneling studies on ultra-thin superconducting films it was shown that the Dynes parameter increases significantly when the film thickness is reduced [1, 2, 41, 42]. This property of ultra-thin films was measured both for NbN films [24, 41] and for MoC films [7]. The proposed explanation is that the interface of the superconducting thin films presents an excess of magnetic impurities, such that for thinner films, their effect on the Dynes in-gap density of states is more pronounced. From our measurements, we conclude that the pair-breaking rate remains small in its magnitude (only few percent of the energy gap) and does not show a systematic dependence on film thickness. Although we do observe a slight increase (excluding the 20 nm sample) in the pair-breaking rate when reducing the film thickness, as seen in the inset of Figure 5(b), the effect is too weak to make a conclusive statement, leaving the question open where the pair-breaking fields predominantly reside within the superconducting film.

V. SUMMARY

We have measured the THz conductivity of five different superconducting NbN thin films with thicknesses ranging from 4.5 to 20 nm. For the thickest sample, we find in the real part of the optical conductivity an absorption onset at $E \approx \Delta$, whose existence has been previously predicted by the Dynes electrodynamics for superconductors as introduced by Herman and Hlubina [5]. Using both time- and frequency-domain THz techniques, we have validated and quantified this excess sub-gap conductivity. Both measurements perfectly complement each other, yielding a temperature-independent pair-breaking rate of $\Gamma \approx 0.036\Delta_0$, and they confirm the necessity of describing the dynamical conductivity of our NbN film using the Dynes formalism. We find equivalent behavior also for thinner NbN films. These results indicate that Dynes scattering is relevant in the THz regime at zero magnetic field, revealing a constant $\Gamma(T)$, in contrast to previous tunneling and point-contact measurements [1, 43]. This suggests that the microscopic processes that underlie the Dynes scattering parameter Γ are more complex than previously thought. At the same time it demonstrates that the Dynes formalism might be the appropriate strategy to quantify sub-gap absorption that does not comply with Mattis-Bardeen predictions [5, 21], in particular for disordered superconductors such as transition-metal nitrides or carbides

[44, 45] that are in the focus of both fundamental research (e.g. the superconductor-insulator transition) and applications (e.g. for superconducting quantum circuitry or cryogenic detectors) [46–48].

ACKNOWLEDGMENTS

We thank M. Ziegler for supporting the sample growth, G. Untereiner for supporting the THz experiments, and C. Beydeda, F. Herman, and J. Pusskeiler for helpful discussions. This work was supported by the Carl-Zeiss-Stiftung as part of CZS Center QPhoton and by the German Federal Ministry of Research, Technology and Space (BMFTR) within project QSolid, Grant No. 13N16159. This work was partially supported by the BMFTR under Grant No. 13N16152/QSolid and “NbNanoQ”, Grant No. 13N17121.

[1] S. P. Chockalingam, M. Chand, A. Kamlapure, J. Jesudasan, A. Mishra, V. Tripathi, and P. Raychaudhuri, Tunneling studies in a homogeneously disordered *s*-wave superconductor: NbN, *Phys. Rev. B* **79**, 094509 (2009).

[2] P. Szabó, T. Samuely, V. Hašková, J. Kačmarčík, M. Žemlička, M. Grajcar, J. G. Rodrigo, and P. Samuely, Fermionic scenario for the destruction of superconductivity in ultrathin MoC films evidenced by STM measurements, *Phys. Rev. B* **93**, 014505 (2016).

[3] T. Proslík, J. F. Zasadzinski, L. Cooley, C. Antoine, J. Moore, J. Norem, M. Pellin, and K. E. Gray, Tunneling study of cavity grade Nb: Possible magnetic scattering at the surface, *Appl. Phys. Lett.* **92**, 212505 (2008).

[4] R. C. Dynes, V. Narayanamurti, and J. P. Garno, Direct measurement of quasiparticle-lifetime broadening in a strong-coupled superconductor, *Phys. Rev. Lett.* **41**, 1509 (1978).

[5] F. Herman and R. Hlubina, Electromagnetic properties of impure superconductors with pair-breaking processes, *Phys. Rev. B* **96**, 014509 (2017).

[6] H. Boschker, E. Fillis-Tsirakis, C. Richter, D. Zhang, J. Smet, and L. Kuerten, Microscopic origin of the dynes parameter Γ of the LaAlO₃–SrTiO₃ interface superconductor, *Phys. Rev. B* **102**, 134506 (2020).

[7] V. Hašková, M. Kopčík, P. Szabó, T. Samuely, J. Kačmarčík, O. Onufriienko, M. Žemlička, P. Neilinger, M. Grajcar, and P. Samuely, On the origin of in-gap states in homogeneously disordered ultrathin films. MoC case, *Appl. Surf. Sci.* **461**, 143 (2018).

[8] D. R. Karecki, G. L. Carr, S. Perkowitz, D. U. Gubser, and S. A. Wolf, Far-infrared conductivity and anomalous below-gap absorption in superconducting granular NbN, *Phys. Rev. B* **27**, 5460 (1983).

[9] K. E. Kornelsen, M. Dressel, J. E. Eldridge, M. J. Brett, and K. L. Westra, Far-infrared optical absorption and reflectivity of a superconducting NbN film, *Phys. Rev. B* **44**, 11882 (1991).

[10] Y. Ikebe, R. Shimano, M. Ikeda, T. Fukumura, and M. Kawasaki, Vortex dynamics in a NbN film studied by terahertz spectroscopy, *Phys. Rev. B* **79**, 174525 (2009).

[11] M. Šindler, R. Tesař, J. Koláček, L. Skrbek, and Z. Šimša, Far-infrared transmission of a superconducting NbN film, *Phys. Rev. B* **81**, 184529 (2010).

[12] M. Beck, M. Klammer, S. Lang, P. Leiderer, V. V. Kabanov, G. N. Gol'tsman, and J. Demsar, Energy-gap dynamics of superconducting NbN thin films studied by time-resolved terahertz spectroscopy, *Phys. Rev. Lett.* **107**, 177007 (2011).

[13] R. Matsunaga and R. Shimano, Nonequilibrium BCS state dynamics induced by intense terahertz pulses in a superconducting NbN film, *Phys. Rev. Lett.* **109**, 187002 (2012).

[14] U. S. Pracht, E. Heintze, C. Clauss, D. Hafner, R. Bek, D. Werner, S. Gelhorn, M. Scheffler, M. Dressel, D. Sherman, B. Gorshunov, K. S. Il'in, D. Henrich, and M. Siegel, Electrodynamics of the superconducting state in ultra-thin films at THz frequencies, *IEEE Trans. THz Sci. Technol.* **3**, 269 (2013).

[15] D. Sherman, U. S. Pracht, B. Gorshunov, S. Poran, J. Jesudasan, M. Chand, P. Raychaudhuri, M. Swanson, N. Trivedi, A. Auerbach, M. Scheffler, A. Frydman, and M. Dressel, The Higgs mode in disordered superconductors close to a quantum phase transition, *Nat. Phys.* **11**, 188 (2015).

[16] B. Cheng, L. Wu, N. J. Laurita, H. Singh, M. Chand, P. Raychaudhuri, and N. P. Armitage, Anomalous gap-edge dissipation in disordered superconductors on the brink of localization, *Phys. Rev. B* **93**, 180511 (2016).

[17] M. Šindler, F. Kadlec, and C. Kadlec, Onset of a superconductor-insulator transition in an ultrathin NbN film under in-plane magnetic field studied by terahertz spectroscopy, *Phys. Rev. B* **105**, 014506 (2022).

[18] S. Linzen, M. Ziegler, O. Astafiev, M. Schmelz, U. Hübner, M. Diegel, E. Il'ichev, and H. Meyer, Structural and electrical properties of ultrathin niobium nitride films grown by atomic layer deposition, *Supercond. Sci. Technol.* **30**, 035010 (2017).

[19] G. K. Deyu, M. Wenskat, I. G. Díaz-Palacio, R. H. Blick, R. Zierold, and W. Hillert, Recent advances in atomic layer deposition of superconducting thin films: a review, *Mater. Horiz.* **12**, 5594 (2025).

[20] U. S. Pracht, N. Bachar, L. Benfatto, G. Deutscher, E. Farber, M. Dressel, and M. Scheffler, Enhanced Cooper pairing versus suppressed phase coherence shaping the superconducting dome in coupled aluminum nanograins, *Phys. Rev. B* **93**, 100503 (2016).

[21] J. Simmendinger, U. S. Pracht, L. Daschke, T. Proslík, J. A. Klug, M. Dressel, and M. Scheffler, Superconducting energy scales and anomalous dissipative conductivity in thin films of molybdenum nitride, *Phys. Rev. B* **94**, 064506 (2016).

[22] L. Kang, B. B. Jin, X. Y. Liu, X. Q. Jia, J. Chen, Z. M. Ji, W. W. Xu, P. H. Wu, S. B. Mi, A. Pimenov, Y. J. Wu, and B. G. Wang, Suppression of superconductivity in epitaxial NbN ultrathin films, *J. Appl. Phys.* **109**, 033908 (2011).

[23] A. Semenov, B. Günther, U. Böttger, H.-W. Hübers, H. Bartolf, A. Engel, A. Schilling, K. Ilin, M. Siegel, R. Schneider, D. Gerthsen, and N. A. Gippius, Optical and transport properties of ultrathin NbN films and nanostructures, *Phys. Rev. B* **80**, 054510 (2009).

[24] A. Kamlapure, M. Mondal, M. Chand, A. Mishra, J. Jesudasan, V. Bagwe, L. Benfatto, V. Tripathi, and P. Raychaudhuri, Measurement of magnetic penetration depth and superconducting energy gap in very thin epitaxial NbN films, *Appl. Phys. Lett.* **96**, 072509 (2010).

[25] Y. Ivry, C.-S. Kim, A. E. Dane, D. De Fazio, A. N. McCaughan, K. A. Sunter, Q. Zhao, and K. K. Berggren, Universal scaling of the critical temperature for thin films near the superconducting-to-insulating transition, *Phys. Rev. B* **90**, 214515 (2014).

[26] T. Bouteiller, A. Marguerite, R. Daou, D. Yakovlev, S. Pons, C. Feuillet-Palma, D. Roditchev, B. Fauqué, and K. Behnia, Nernst effect and its thickness dependence in superconducting NbN films, *Phys. Rev. Mater.* **9**, 094807 (2025).

[27] W. Zimmermann, E. Brandt, M. Bauer, E. Seider, and L. Genzel, Optical conductivity of bcs superconductors with arbitrary purity, *Phys. C: Supercond.* **183**, 99 (1991).

[28] M. Dressel and G. Grüner, *Electrodynamics of solids: Optical properties of electrons in matter* (Cambridge University Press, 2002).

[29] K. Steinberg, M. Scheffler, and M. Dressel, Quasiparticle response of superconducting aluminum to electromagnetic radiation, *Phys. Rev. B* **77**, 214517 (2008).

[30] C. Carbillot, V. Cherkez, M. A. Skvortsov, M. V. Feigel'man, F. Debontridder, L. B. Ioffe, V. S. Stolyarov, K. Ilin, M. Siegel, D. Roditchev, T. Cren, and C. Brun, Spectroscopic evidence for strong correlations between local superconducting gap and local altshuler-aronov density of states suppression in ultrathin NbN films, *Phys. Rev. B* **102**, 024504 (2020).

[31] S. Dutta, P. Raychaudhuri, S. S. Mandal, and T. V. Ramakrishnan, Superfluid density in conventional superconductors: from clean to strongly disordered, *J. Condens. Matter Phys.* **34**, 335601 (2022).

[32] D. Henrich, S. Dörner, M. Hofherr, K. Il'in, A. Semenov, E. Heintze, M. Scheffler, M. Dressel, and M. Siegel, Broadening of hot-spot response spectrum of superconducting NbN nanowire single-photon detector with reduced nitrogen content, *J. Appl. Phys.* **112**, 074511 (2012).

[33] M. Chand, G. Saraswat, A. Kamlapure, M. Mondal, S. Kumar, J. Jesudasan, V. Bagwe, L. Benfatto, V. Tripathi, and P. Raychaudhuri, Phase diagram of the strongly disordered *s*-wave superconductor NbN close to the metal-insulator transition, *Phys. Rev. B* **85**, 014508 (2012).

[34] A. Kamlapure, T. Das, S. C. Ganguli, J. B. Parmar, S. Bhattacharyya, and P. Raychaudhuri, Emergence of nanoscale inhomogeneity in the superconducting state of a homogeneously disordered conventional superconductor, *Sci. Rep.* **3**, 2979 (2013).

[35] B. Sacépé, T. Dubouchet, C. Chapelier, M. Sanquer, M. Ovadia, D. Shahar, M. Feigel'man, and L. Ioffe, Localization of preformed Cooper pairs in disordered superconductors, *Nat. Phys.* **7**, 239 (2011).

[36] S. B. Kaplan, C. C. Chi, D. N. Langenberg, J. J. Chang, S. Jafarey, and D. J. Scalapino, Quasiparticle and phonon lifetimes in superconductors, *Phys. Rev. B* **14**, 4854 (1976).

[37] A. Mikhailovsky, S. Shulga, A. Karakozov, O. Dolgov, and E. Maksimov, Thermal pair-breaking in superconductors with strong electron-phonon interaction, *Solid State Commun.* **80**, 511 (1991).

[38] F. Herman and R. Hlubina, Microscopic interpretation of the Dynes formula for the tunneling density of states, *Phys. Rev. B* **94**, 144508 (2016).

[39] F. Herman and R. Hlubina, Thermodynamic properties of Dynes superconductors, *Phys. Rev. B* **97**, 014517 (2018).

[40] F. Yang and M. W. Wu, Diamagnetic property and optical absorption of conventional superconductors with magnetic impurities in linear response, *Phys. Rev. B* **109**, 064508 (2024).

[41] Y. Noat, V. Cherkez, C. Brun, T. Cren, C. Carbillot, F. Debontridder, K. Ilin, M. Siegel, A. Semenov, H.-W. Hübers, and D. Roditchev, Unconventional superconductivity in ultrathin superconducting NbN films studied by scanning tunneling spectroscopy, *Phys. Rev. B* **88**, 014503 (2013).

[42] I. Tamir, M. Trahms, F. Gorniaczyk, F. von Oppen, D. Shahar, and K. J. Franke, Direct observation of intrinsic surface magnetic disorder in amorphous superconducting films, *Phys. Rev. B* **105**, L140505 (2022).

[43] Y. F. Wu, A. B. Yu, L. B. Lei, C. Zhang, T. Wang, Y. H. Ma, Z. Huang, L. X. Chen, Y. S. Liu, C. M. Schneider, G. Mu, H. Xiao, and T. Hu, Superconducting nbn and $\text{cafe}_0.88\text{co}_0.12\text{AsF}$ studied by point-contact spectroscopy with a nanoparticle au array, *Phys. Rev. B* **101**, 174502 (2020).

[44] M. Baránek, P. Neilinger, D. Manca, O. G. Turutanov, and M. Grajcar, Conductivity of strongly disordered ultra-thin moc superconducting films investigated by transmission line spectroscopy, *Physica C* **635**, 1354749 (2025).

[45] O. Saritas, F. Bolle, Y. Lin, M. Dressel, R. Potjan, M. Wislicenus, A. Reck, and M. Scheffler, THz electrodynamics and superconducting energy scales of ZrN thin films, *Appl. Phys. Lett.* **127**, 192601 (2025).

[46] W. D. Oliver and P. B. Welander, Materials in superconducting quantum bits, *MRS Bulletin* **38**, 816–825 (2013).

[47] I. Esmaeil Zadeh, J. Chang, J. W. N. Los, S. Gyger, A. W. Elshaari, S. Steinhauer, S. N. Dorenbos, and V. Zwiller, Superconducting nanowire single-photon detectors: A perspective on evolution, state-of-the-art, future developments, and applications, *Appl. Phys. Lett.* **118**, 190502 (2021).

[48] D. Wang, Y. Wu, N. Pieczulewski, P. Garg, M. C. C. Pace, C. G. L. Böttcher, B. Mazumder, D. A. Muller, and H. X. Tang, All-nitride superconducting qubits based on atomic layer deposition, *Nat. Mater.* (2026).